High Reynolds Channel Flows: Variable curvature

M. Zagzoule[1], P. Cathalifaud[1], J. Cousteix[2], and J. Mauss[1]

[1] Université de Toulouse ; INPT, UPS ; CNRS ; IMFT ; F-31400 Toulouse, France
zagzoule@imft.fr, catalifo@imft.fr, mauss@cict.fr
[2] DMAE, ONERA, ISAE; Toulouse, France Jean.Cousteix@onecert.fr

Summary. Two-dimensional laminar flow, at high Reynolds number Re, of an incompressible Newtonian fluid in a curved channel connected to 2 fitting tangent straight channels at its upstream and downstream extremities is considered. The Successive Complementary Expansion Method (SCEM) is adopted. This method leads to an asymptotic reduced model called Global Interactive Boundary Layer (GIBL) which gives a uniformly valid approximate solution of the flow field in the whole domain. To explore the effect of the variable curvature on the flow field, the bend has an elliptical median line. The validity of the proposed GIBL model is confronted to the numerical solution of complete Navier- Stokes equations. This comparison includes the wall shear stress which is a very sensitive measure of the flow field. The GIBL results match very well the complete Navier-stokes results for curvatures K_{max} up to 0.4, curvature variations $|K'_{max}|$ up to 0.7 and eccentricities e up to $\simeq 0.943$ in the whole geometrical domain. The upstream and downstream effects as well as the impact of the curvature discontinuities and the behaviour in the entire bend are well captured by the GIBL model.

1 Mathematical Formulation

1.1 Geometrical configuration

As a typical illustration we consider a 2D bend connected to 2 fitting tangent straight channels at its upstream and downstream extremities (see figure 1). The bend starts at $x = 0$, the median line is denoted $H(x, y) = 0$. Generalized coordinates (X, Y) are used and are defined such that: X and Y are distances along and perpendicular to $H = 0$ with the wall boundaries located at $Y = \pm 1/2$. In the straight parts this coordinate system reduces to the Cartesian one (x, y). The velocity components U and V are respectively parallel and perpendicular to $H = 0$, thus

$$\mathbf{V} = U\boldsymbol{\tau} + V\mathbf{n}\ , \quad \text{where} \quad \boldsymbol{\tau} = \mathbf{X} \text{ and } \mathbf{n} = \mathbf{Y}\ .$$

$\boldsymbol{\tau}$ and $\mathbf{n}$ are unit vectors respectively tangent and normal to the median line. $K(X)$ is the algebraic curvature of the median line. Since $(\boldsymbol{\tau}, \mathbf{n})$ is direct, hence $K < 0$ in the case of figure 1.

1.2 Navier-Stokes equations in generalized coordinates

In the previously defined generalized coordinate system the continuity equation and the Cauchy equations are

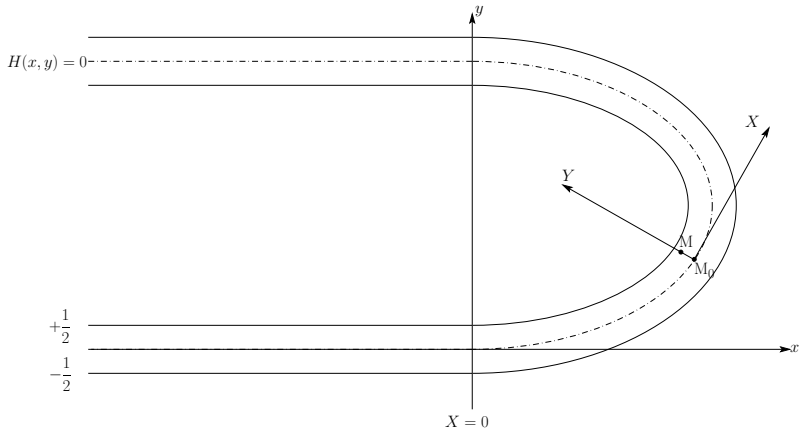

Fig. 1. Geometrical configuration and coordinate system.

$$\frac{\partial U}{\partial X} + \frac{\partial}{\partial Y}\left[(1+KY)V\right] = 0$$

$$\frac{1}{1+KY}U\frac{\partial U}{\partial X} + V\frac{\partial U}{\partial Y} + K\frac{UV}{1+KY} = -\frac{1}{1+KY}\frac{\partial P}{\partial X} + \frac{1}{1+KY}\left[\frac{\partial \sigma_{XX}}{\partial X} + \frac{\partial}{\partial Y}(1+KY)\sigma_{XY} + K\sigma_{XY}\right]$$

$$\frac{1}{1+KY}U\frac{\partial V}{\partial X} + V\frac{\partial V}{\partial Y} - \frac{K}{1+KY}U^2 = -\frac{\partial P}{\partial Y} + \frac{1}{1+KY}\left[\frac{\partial \sigma_{XY}}{\partial X} + \frac{\partial}{\partial Y}(1+KY)\sigma_{XY} - K\sigma_{XX}\right]$$

where, for a newtonian fluid

$$\sigma_{XX} = \frac{2}{(1+KY)R_e}\left(\frac{\partial U}{\partial X} + KV\right)$$

$$\sigma_{XY} = \frac{1}{(1+KY)R_e}\left(\frac{\partial V}{\partial X} + (1+KY)\frac{\partial U}{\partial Y} - KU\right)$$

$$\sigma_{YY} = \frac{2}{R_e}\frac{\partial V}{\partial Y}$$

The Reynolds number R_e is given by $R_e = \frac{\rho\, U^* H^*}{\mu^*}$, where U^* and H^* are characteristic velocity and length, ρ the density and μ^* the viscosity.

These equations must be solved with boundary conditions,

$$U = V = 0 \quad \text{for} \quad Y = \pm 1/2$$

1.3 The O(δ) Navier-Stokes equations

The variable curvature $K = \delta k(X)$ and its variation in X are now considered small, δ being a small positive parameter. Since we are considering a high Reynolds number basic flow dominated by its longitudinal component, all the terms are small except U, $\dfrac{\partial U}{\partial Y}$ and $\dfrac{\partial^2 U}{\partial Y^2}$ which are of order 1. Then, to order δ included, continuity equation and Navier-Stokes equations can be written in the stationary case,

$$\frac{\partial U}{\partial X} + \frac{\partial V}{\partial Y} = 0 \tag{1}$$

$$U\frac{\partial U}{\partial X} + V\frac{\partial U}{\partial Y} + \frac{\partial P}{\partial X} - \frac{1}{R_e}\left(\frac{\partial^2 U}{\partial X^2} + \frac{\partial}{\partial Y}\left[(1+KY)\frac{\partial U}{\partial Y}\right]\right) = 0 \tag{2}$$

$$U\frac{\partial V}{\partial X} + V\frac{\partial V}{\partial Y} - KU^2 + \frac{\partial P}{\partial Y} - \frac{1}{R_e}\left(\frac{\partial^2 V}{\partial X^2} + \frac{\partial^2 V}{\partial Y^2}\right) = 0 \tag{3}$$

Note that in this O(δ) approximation the curvature is appearing only twice : in the viscous term of the longitudinal momentum equation as a "variable viscosity" and in the KU^2 centrifugal / inertial part of the transversal momentum equation. The streamline curvature creates a radial pressure gradient which is very important for upstream influence. To simplify the notation the unknowns are still denoted (U, V, P), even if now it is a *uniformly valid approximation*.

1.4 The GIBL model for a curved channel

A - Velocity field

We seek a solution in the form: $U = u_0 + \delta u$, $V = \delta v$, where $u_0(Y) = \frac{1}{4} - Y^2$ is the basic unperturbed Poiseuille flow.

According to the Successive Complementary Expansion Method (SCEM), developed by [3], the core approximation,

$$U = u_0(Y) + \delta u_1(X, Y, \delta) + \dots \,, \tag{4}$$

$$V = \delta v_1(X, Y, \delta) + \dots \,, \tag{5}$$

can be complemented to build a Uniformly Valid Approximation (UVA) [4] :

$$U = u_0(Y) + \delta\left(u_1(X, Y, \delta) + U_{BL}^{+}(X, \eta^{+}, \delta) + U_{BL}^{-}(X, \eta^{-}, \delta)\right) \tag{6}$$

$$V = \delta\left(v_1(X, Y, \delta) + \varepsilon[V_{BL}^{+}(X, \eta^{+}, \delta) + V_{BL}^{-}(X, \eta^{-}, \delta)]\right) \tag{7}$$

the dependence on the Reynolds number being implicit; the terms U_{BL} and V_{BL}, being of order 1, are correcting terms respectively to u_1 and v_1 in the upper and lower boundary layers such that, $\lim_{\eta\to\infty} U_{BL} = 0$, and $\lim_{\eta\to\infty} V_{BL} = 0$. The boundary layer variables $\eta^{\pm}$ are given by, $\eta^{+} = \frac{\frac{1}{2}-Y}{\varepsilon}$ and $\eta^{-} = \frac{\frac{1}{2}+Y}{\varepsilon}$. The form of V is imposed by the continuity equation. In the longitudinal equation, in order to have the same order for the inertial and viscous terms and since $u_0 = \mathrm{O}(\varepsilon)$ in the boundary layer, we take $\varepsilon = \mathrm{O}_S\left(R_e^{-\frac{1}{3}}\right)$. The first significant perturbation is obtained when, in the

boundary layer, ε and δ are of the same order, i.e. $\delta = \mathrm{O}\left(R_e^{-\frac{1}{3}}\right)$, which allows U to be negative. A characteristic number that links the Reynolds number R_e and the curvature δ is thus defined by $\mu = \delta R_e^{\frac{1}{3}}$. The parameter μ can be seen as the ratio between the curvature δ and the boundary layer thickness ε. The challenging case is therefore μ being $\mathrm{O}(1)$, which is our assumption.

B - Pressure field

In the core flow $P = p_0(X) + \delta p_1(X, Y, \delta) + \ldots$. Then a UVA for the pressure is as follows:

$$P = p_0(X) + \delta \left[p_1(X, Y, \delta) + \Delta(\varepsilon)(P_{BL}^+(X, \eta^+, \delta) + P_{BL}^-(X, \eta^-, \delta)) \right]$$

where the P_{BL} terms satisfy $\lim_{\eta \to \infty} P_{BL} = 0$ and $\Delta(\varepsilon)$ is a gauge function not yet determined. A careful analysis of the various orders of magnitude [8], in the core flow, and especially in the boundary layer, shows that $\Delta = \mathrm{O}(\varepsilon^3)$. Now, from equation (3), it can be seen that in the whole field, boundary layer and core, we have the key result,

$$\frac{\partial P}{\partial X} = \frac{\mathrm{d}p_0}{\mathrm{d}X} + \delta \left(\frac{\partial p_1}{\partial X} + \mathrm{O}(\varepsilon^3) \right) \tag{8}$$

Thus at the considered order, in equation (2), $\dfrac{\partial P}{\partial X}$ can be replaced by $\dfrac{\partial P_1}{\partial X}$, given by:

$$\frac{\partial P_1}{\partial X} = \frac{\mathrm{d}p_0}{\mathrm{d}X} + \delta \frac{\partial p_1}{\partial X} \, . \tag{9}$$

The long scale approximation [6, 7] yields a simplified model for the pressure gradient [8] :

$$\frac{\partial P_1}{\partial X} = \frac{\mathrm{d}p_0}{\mathrm{d}X} + \delta \left(A''' + k' \right) \int_{\eta_c}^{\eta} u_0^2(\eta') \, \mathrm{d}\eta' \quad + \delta B'(X) \tag{10}$$

where A is the so called displacement function, $(u_1 = A(X) u_0' \, , \quad v_1 = -u_0 A'(X))$.

C - GIBL

Finally the global interactive boundary layer model (GIBL) for the straight and variable curved channel parts consists of the generalized boundary layer equations :

$$\frac{\partial U}{\partial X} + \frac{\partial V}{\partial Y} = 0 \tag{11}$$

$$U \frac{\partial U}{\partial X} + V \frac{\partial U}{\partial Y} = -\frac{\partial P_1}{\partial X} + \frac{1}{R_e} \frac{\partial}{\partial Y} \left[(1 + KY) \frac{\partial U}{\partial Y} \right] \tag{12}$$

$$\text{where} \quad \frac{\partial P_1}{\partial X} = \frac{\mathrm{d}p_0}{\mathrm{d}X} + \delta \left(A''' + k' \right) \int_{\eta_c}^{\eta} u_0^2(\eta') \, \mathrm{d}\eta' \quad + \delta B'(X)$$

with $U = V = 0 \quad$ for $\quad Y = \pm 1/2$. This model is uniformly valid in the whole flow field , involving U and V instead of their boundary layers values U_{BL} and V_{BL}. Consequently we have in the core flow $V = V_1$ where, in the case of the long scale approximation, $V1 = -\delta u_0 A'(X)$.

Thus using this last relation as a coupling condition imposed at the median line the numerical resolution of the GIBL model is done through an iterative procedure in which the calculation domain is swept from upstream to downstream.The sweeping is repeated until convergence is achieved on A and B and finally on the shear stress. See [1, 8] for more details.

2 Results and discussion

Figures 2 to 4 present several cases where the wall shear stress ($C_f = \mp \frac{2}{R_e} \left.\frac{\partial U}{\partial Y}\right|_{Y=\pm\frac{1}{2}}$) as obtained by the GIBL model is compared to the numerical solution of the complete Navier-Stokes equations for $R_e = 1000$. At the inlet of the upstream straight tangent channel a parabolic profile was given while at the outlet of the downstream channel a constant zero pressure was prescribed. The GIBL results match very well the complete Navier-stokes results for K_{max} up to 0.4 and the eccentricity e up to $\simeq 0.943$ in the whole geometrical domain. The upstream and downstream effects as well as the impact of the curvature discontinuities at the junctions are well captured, and the behaviour in the entire bend is quantitatively well reproduced by the GIBL model .

The behaviour of the wall shear stress in the upstream tangent channel is similar to the case of a distal constant curvature bend [8]: some distance ahead from the junction with the bend the normalised shear stress increases at the internal wall and decreases at the external wall relatively to the upstream Poiseuille flow. The length of this upstream influence to an incoming Poiseuille flow was shown asymptotically by Smith[5] to be, for high Reynolds, of the order of $R_e^{\frac{1}{7}}$ whatever the nature of the distal perturbation is. In a companion paper [2] this result is confirmed numerically and by a modal analysis.

In the tree cases tested the median line curvature $K(X)$ increases up to the middle of the bend where $K_{max}$is reached and then decreases, while the maximum of its variation K'_{max} is reached just before the middle of the bend. Both $K(X)$ and $K'(X)$ combined to the fluid inertia modulate the shape and the peaks of the internal and external wall shear stresses. The wall shear stress peaks are attained just before the middle of the bend.

Figure 2 shows the case of a channel having an elliptical median line that deviates little from a circle, with its major semi-axis $a = 10$ and its minor semi-axis $b = 8$, hence an eccentricity $e = 0.6$. For a circular bend of radius equal to 10, thus having a constant curvature $\delta = 0.1$, an established flow occurs in the bend at the same Reynolds number, that is a constant value of the shear stress is attained and maintained in a large part of the bend away from the discontinuities [8]. On the contrary it is seen here that a small deviation from a circular median line, i.e. a small variable curvature with $K_{max} \simeq 0.16$ and $|K'_{max}| \simeq 0.08$, has a clear influence in the spatial evolution of the wall shear stress. No constant wall shear stress is to be expected when the curvature varies as can be clearly deduced from the pressure gradient expression of equation (10) which is a function of the curvature variation $K'(X)$, not to mention the viscous term since $K = \delta k'(X)$ in the longitudinal momentum equation (12). In the case of figure 2, the wall shear stress peaks just before the middle of the bend are less than those induced by the discontinuities at the upstream and downstream junctions with the straight tangent channels.

In figure 3 the ellipticity of the median line is increased with $K_{max} = 0.4$, $|K'_{max}| \simeq 0.6$ and $e \simeq 0.866$. Here the peaks of the shear stress inside the bend are larger than those which occur at the discontinuities. The key parameter μ is now equal to 4 leading to slight differences in the wall shear stress peaks inside the bend between the GIBL model and the complete Navier-Stokes equations results.

To isolate more the variable curvature effects from those induced by the discontinuities of the junctions in one hand and to test the GIBL model validity with a stronger eccentricity on the other hand we run the case of figure 3 where $e \simeq 0.943$ with $K_{max} \simeq 0.3$ and $|K'_{max}| \simeq 0.7$. Here the junction discontinuities are smaller than the previous cases and $\mu = 3$.

The GIBL accuracy is mainly dependent on the key parameter $\mu = \delta R_e^{\frac{1}{3}}$ since this asymptotic model has been built under the assumption that μ is O(*1*) . Not presented in the present work,

quite good agreement is achieved even when $\mu \simeq 11$, i.e. when $K_{max} \simeq 1.1$ and $K'_{max} \simeq 3$, which is out of the formal range of validity of the GIBL model.

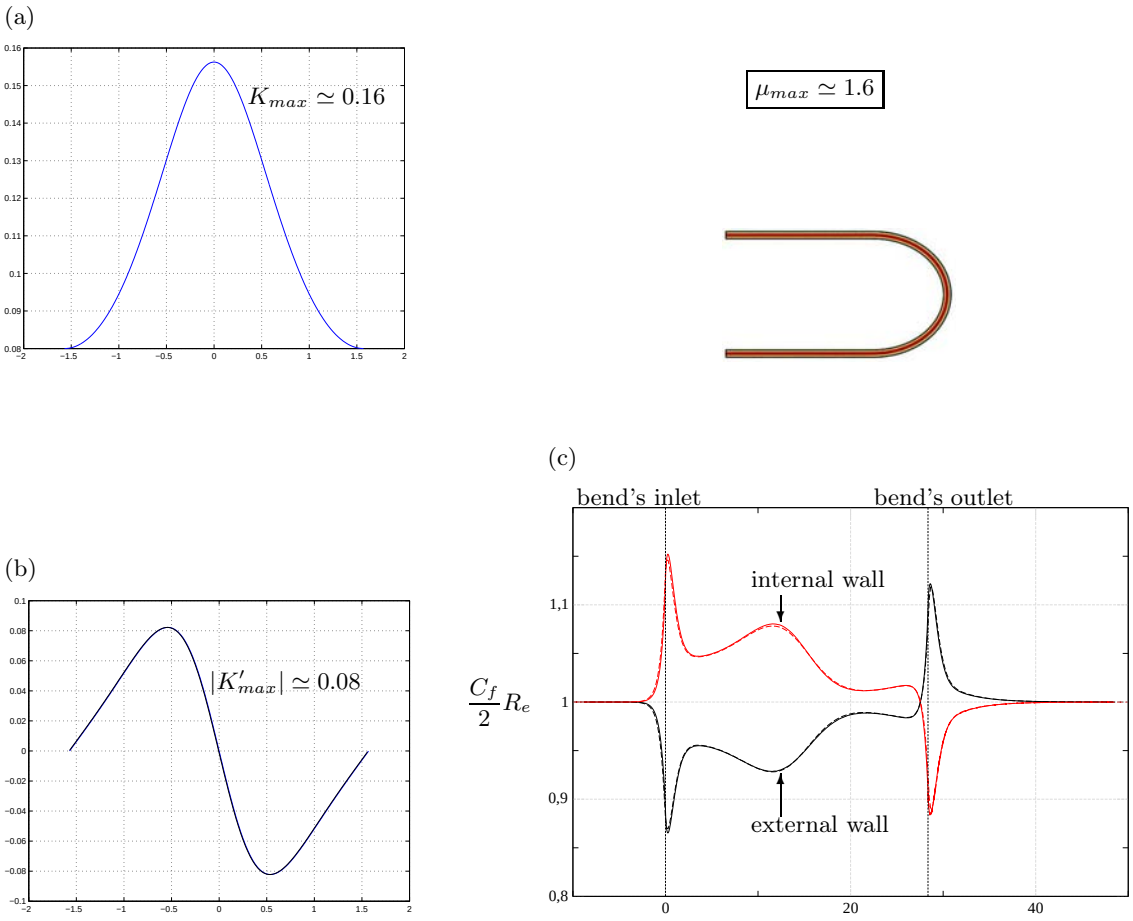

Fig. 2. Elliptical bend $[-\pi/2, \pi/2]$; $R_e = 1000$, major semi-axis $a = 10$, minor semi-axis $b = 8$, eccentricity $e = 0.6$; (a): Median line curvature K evolution; (b): dK/dX evolution; (c) Wall shear stress; straight lines: NS results; dashed lines: GIBL results.

References

1. P. Cathalifaud, J. Mauss, and J. Cousteix. Nonlinear aspects of high reynolds number channel flow. *Eur. J. of Mech. B/Fluids*, 29 (4):295–304, 2010.
2. P. Cathalifaud, M. Zagzoule, J. Cousteix, and J. Mauss. High reynolds channel flows: Upstream interaction of various wall deformations. *Lecture Notes in Computational Science and Engineering*, 2011.
3. J. Cousteix and J. Mauss. *Asymptotic analysis and boundary layers*, volume XVIII, Scientific Computation. Springer, Berlin, Heidelberg, 2007.

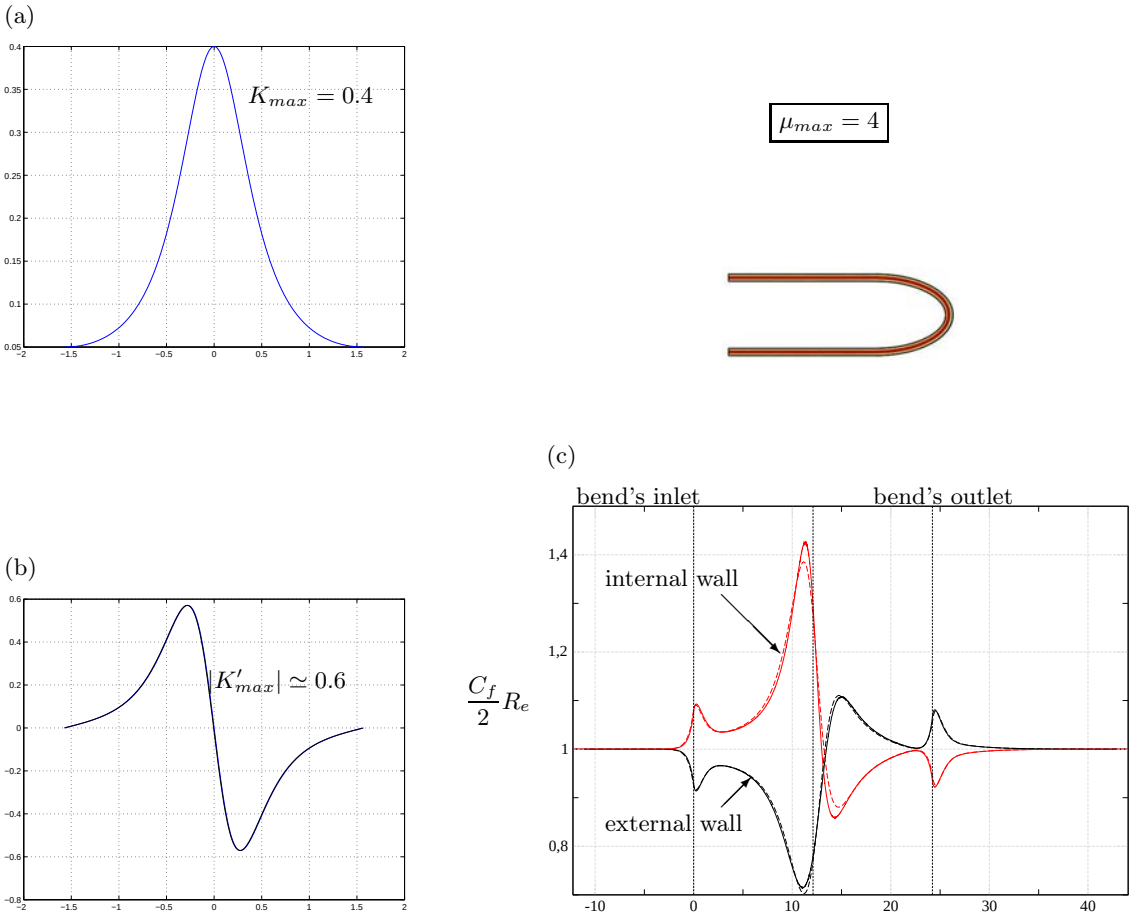

Fig. 3. Elliptical bend $[-\pi/2, \pi/2]$; $R_e = 1000$, major semi-axis $a = 10$, minor semi-axis $b = 5$, eccentricity $e \simeq 0.866$; (a): Median line curvature K evolution; (b): dK/dX evolution; (c) Wall shear stress; straight lines: NS results; dashed lines: GIBL results.

4. J. Cousteix and J. Mauss. Interactive boundary layer models for channel flow. *Eur. J. of Mech. B/Fluids*, 28:72–87, 2009.
5. F. T. Smith. Upstream interactions in channel flows. *Journal of Fluid Mechanics*, 79:631–655, 1977.
6. F. T. Smith. On the high reynolds number theory of laminar flows. *IMA J. Appl. Math.*, 28 (3):207–281, 1982.
7. K. Stewartson and P. G. Williams. Self induced separation. *Proc. Roy. Soc. London*, A312:181–206, 1969.
8. M. Zagzoule, P. Cathalifaud, J. Cousteix, and J. Mauss. Uniformly valid asymptotic flow analysis in curved channels. *submitted to Physics of fluids*, 2010.

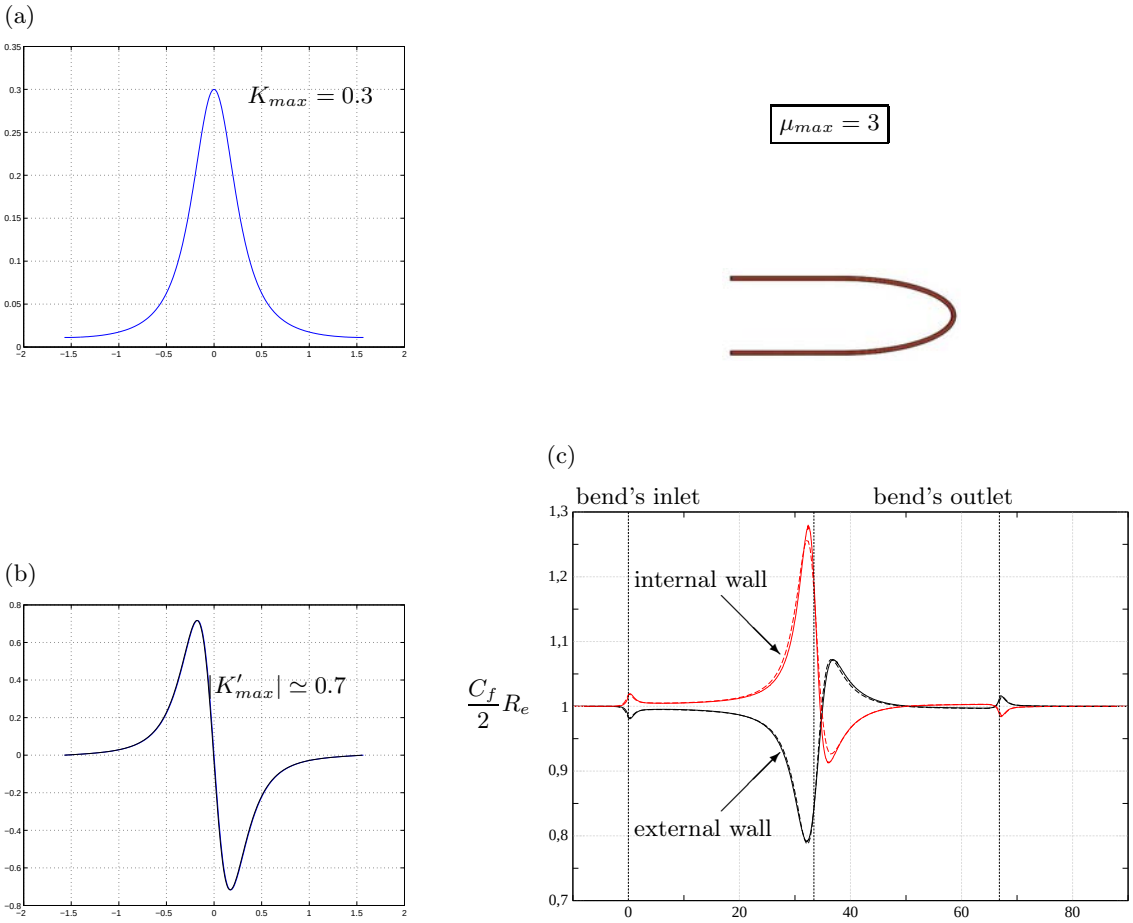

Fig. 4. Elliptical bend $[-\pi/2, \pi/2]$; $R_e = 1000$, major semi-axis $a = 30$, minor semi-axis $b = 10$, eccentricity $e \simeq 0.943$; (a): Median line curvature K evolution; (b): dK/dX evolution; (c) Wall shear stress; straight lines: NS results; dashed lines: GIBL results.